Electronic Supplementary Information for

Evaluation of Attractive Interactions in the Second Coordination Sphere of Iron Complexes Containing Pendant Amines

Qian Liao, Tianbiao Liu, Samantha I. Johnson, Christina M. Klug, Eric S. Wiedner,*
R. Morris Bullock, and Daniel L. DuBois

Center for Molecular Electrocatalysis, Pacific Northwest National Laboratory, P.O. Box 999, K2-57, Richland, WA 99352 United States. E-mail: eric.wiedner@pnnl.gov

Table of Contents ***Page***

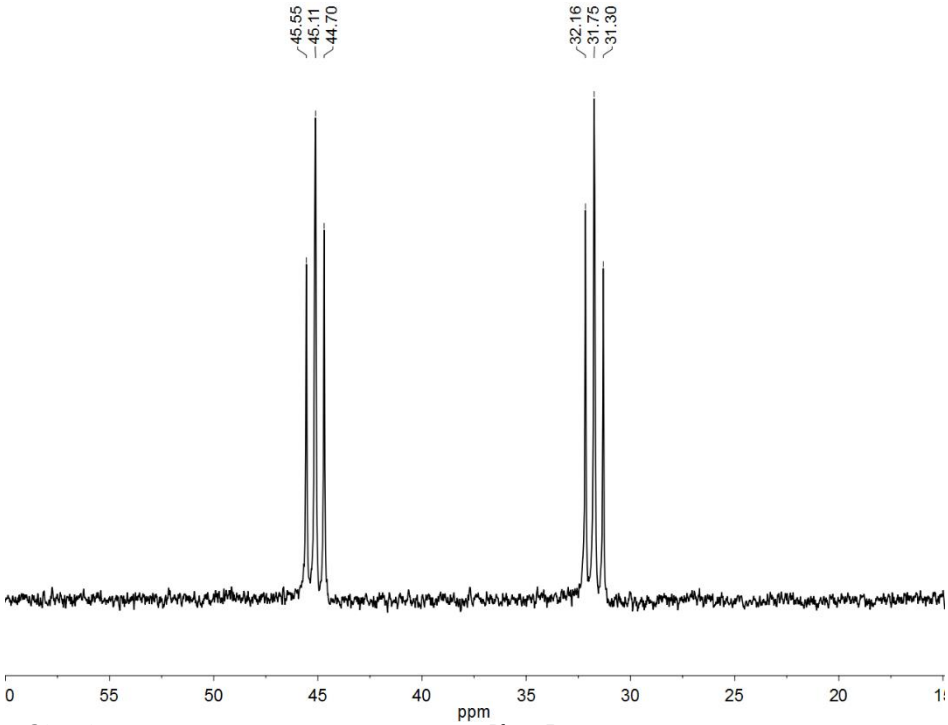

Figure S1. $^{31}P\{^{1}H\}$ NMR spectrum of *cis*-Fe($P^{Ph}_2N^{Bn}_2$)$_2$Cl$_2$ in C_6D_5Cl at 20 °C.

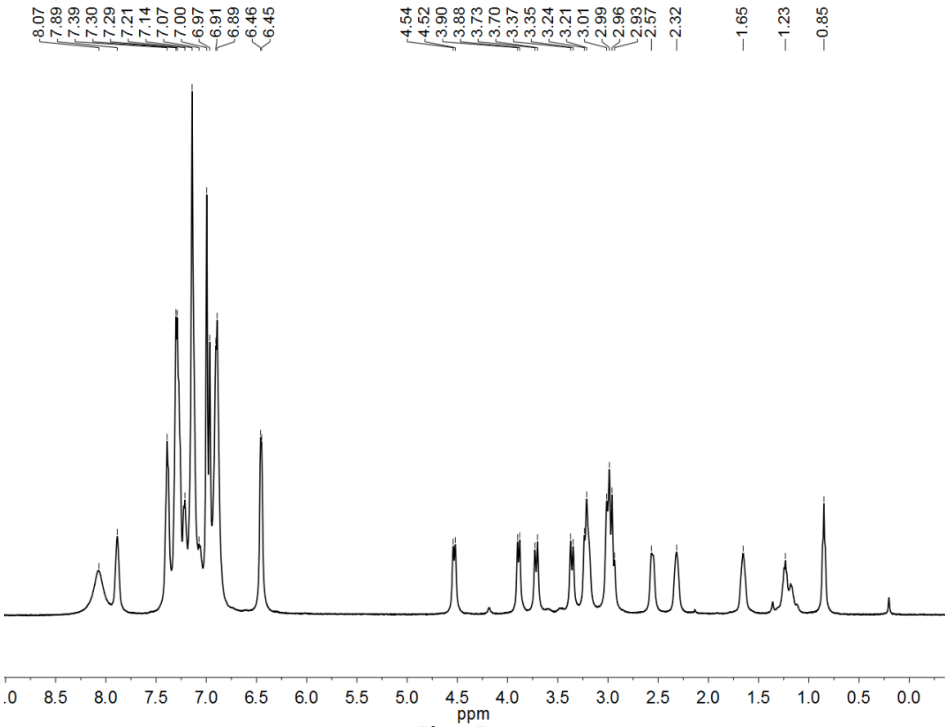

Figure S2. ^{1}H NMR spectrum of *cis*-Fe($P^{Ph}_2N^{Bn}_2$)$_2$Cl$_2$ in C_6D_5Cl at –27 °C. Resonances at 0.85 and 1.23 ppm are attributed to residual pentane.

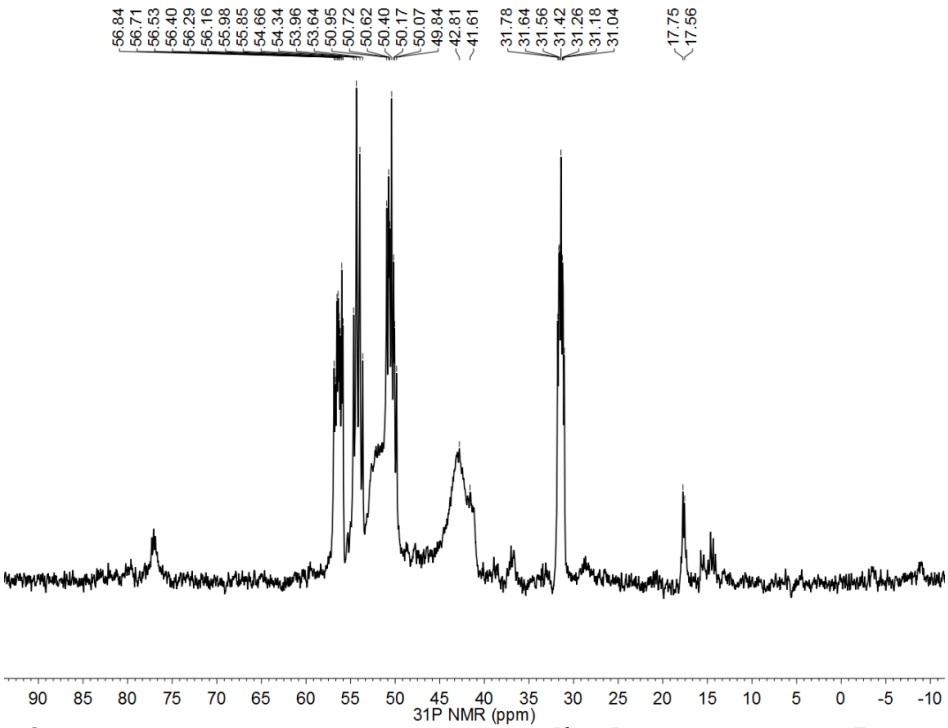

Figure S3. $^{31}P\{^{1}H\}$ NMR spectrum of *trans*-[HFe($P^{Ph}_2N^{Bn}_2$)$_2$(CH_3CN)]BAr^F_4 in C_6D_5Cl at 20 °C.

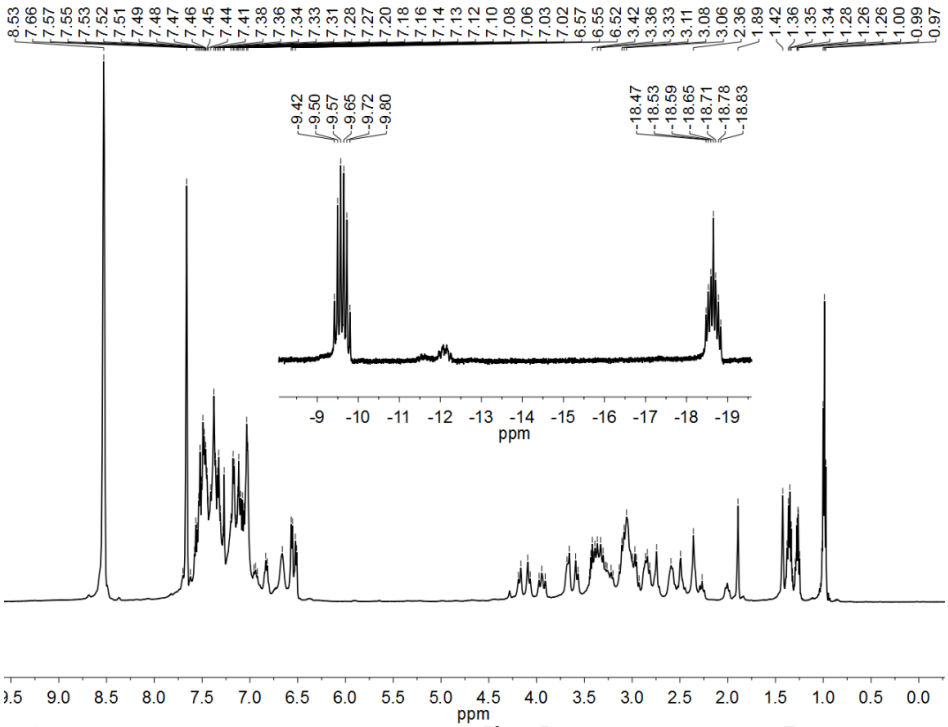

Figure S4. ^{1}H NMR spectrum of *trans*-[HFe($P^{Ph}_2N^{Bn}_2$)$_2$(CH_3CN)]BAr^F_4 in C_6D_5Cl at –27 °C. Inset: Zoom-in of hydride resonance

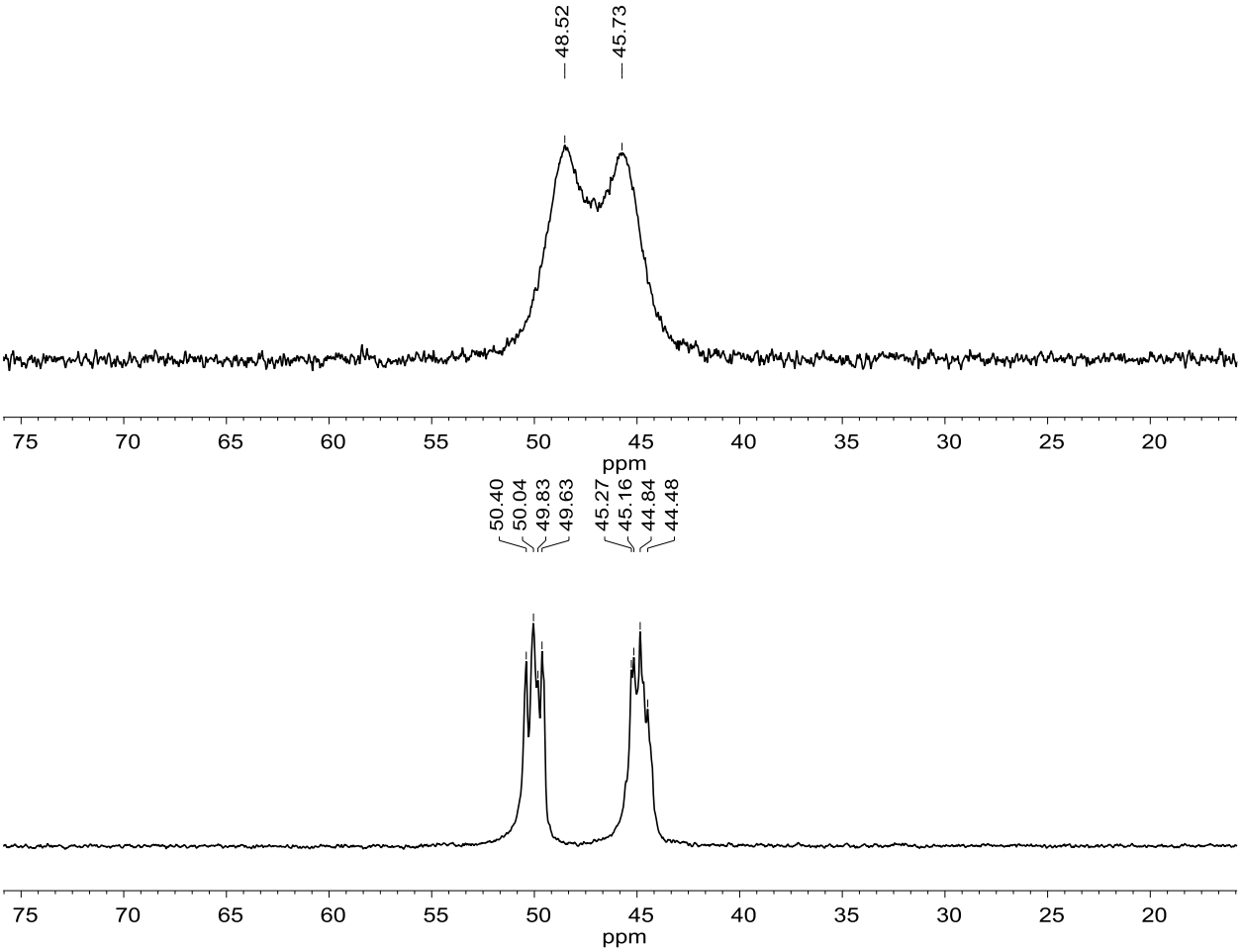

Figure S5. $^{31}P\{^{1}H\}$ NMR spectrum of *trans*-$HFe(P^{Ph}{}_2N^{Bn}{}_2)_2Cl$ in C_6D_5Cl at 20 °C (top) and -27 °C (bottom).

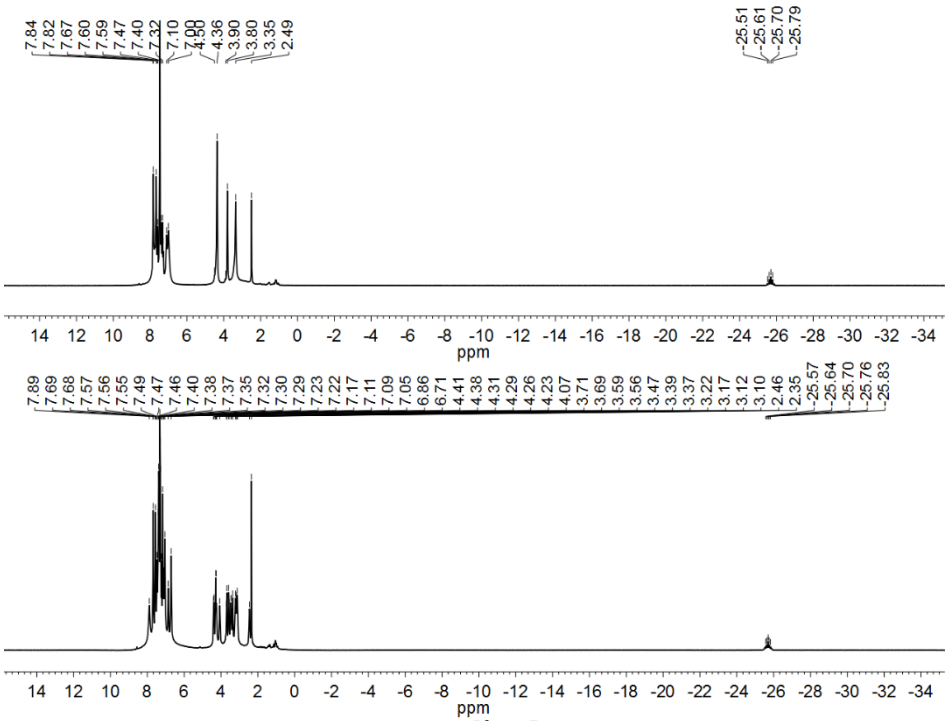

Figure S6. ^{1}H NMR spectrum of *trans*-HFe($P^{Ph}_2N^{Bn}_2$)$_2$Cl in C_6D_5Cl at 25 °C (top) and –27 °C (bottom).

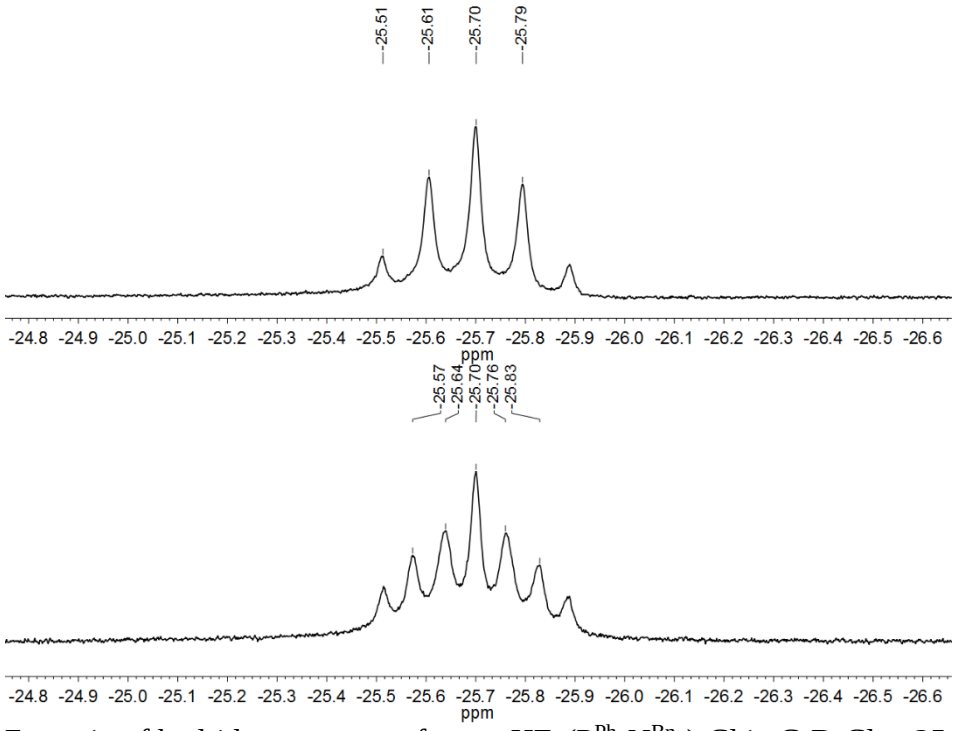

Figure S7. Zoom-in of hydride resonance of *trans*-HFe($P^{Ph}_2N^{Bn}_2$)$_2$Cl in C_6D_5Cl at 25 °C (top) and –27 °C (bottom).

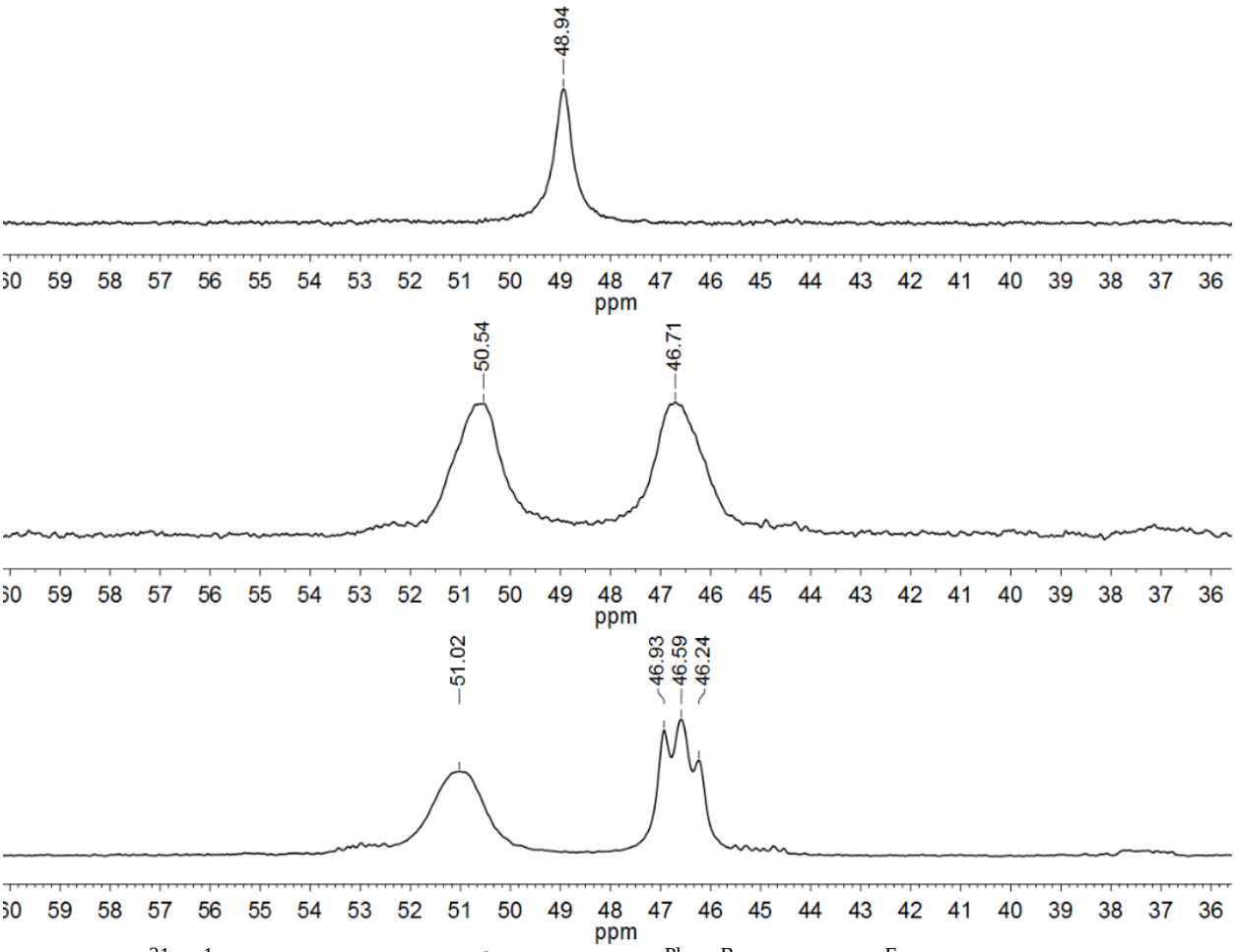

Figure S8. $^{31}P\{^{1}H\}$ NMR spectrum of *trans*-[HFe($P^{Ph}_2N^{Bn}_2$)$_2$CO]BAr^F_4 in C_6D_5Cl at 80 °C (top), 25 °C (middle), and –27 °C (bottom).

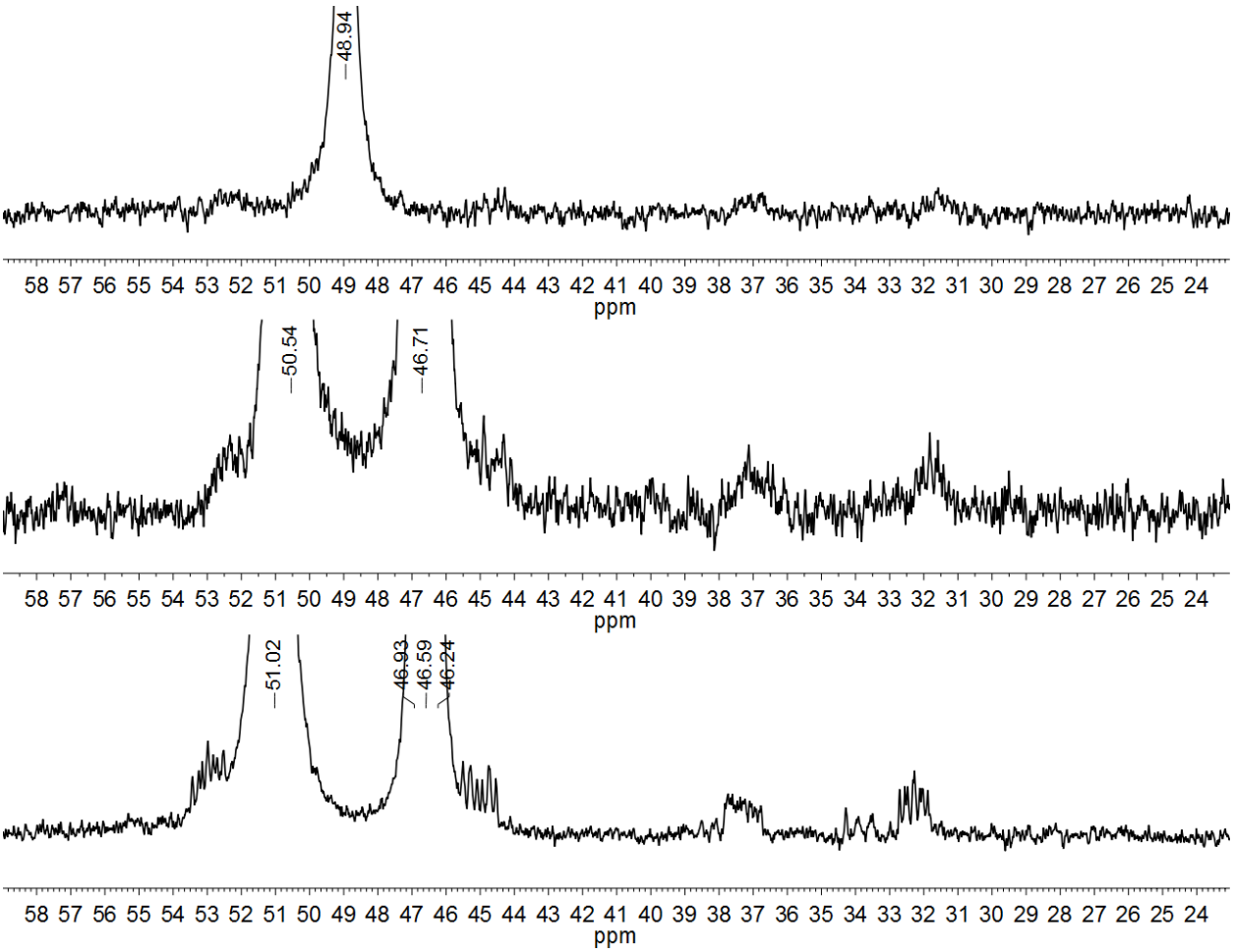

Figure S9. Zoomed-in $^{31}P\{^{1}H\}$ NMR spectrum of *trans*-[HFe($P^{Ph}_2N^{Bn}_2$)$_2$CO]BAr^F_4 in C_6D_5Cl at 80 °C (top), 25 °C (middle), and –27 °C (bottom) highlighting cis isomers.

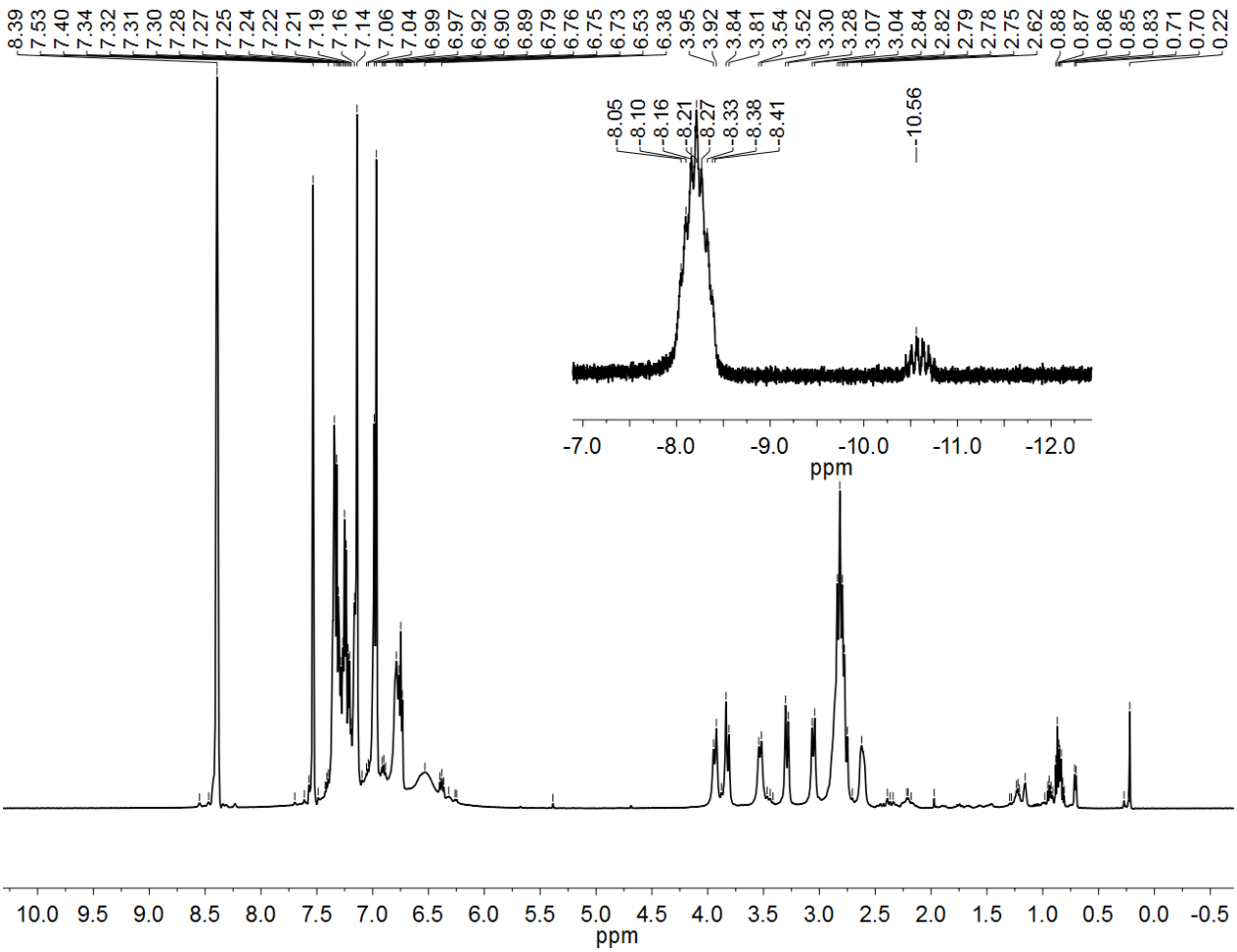

Figure S10. ^{1}H NMR spectrum of *trans*-[HFe($P^{Ph}_2N^{Bn}_2$)$_2$CO]BAr^F_4 in C_6D_5Cl at –27 °C. Inset: Zoom-in of hydride resonances.

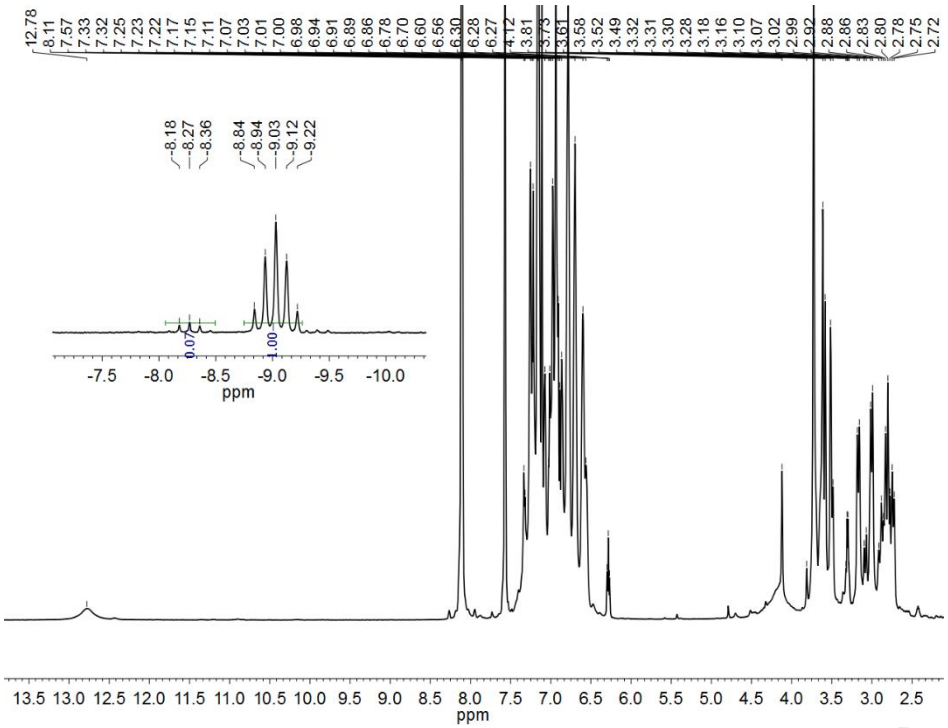

Figure S11. ^{1}H NMR spectrum of reaction between 2,6-dichloroanilinium BAr^{F}_{4} and *trans*-[HFe($P^{Ph}_{2}N^{Bn}_{2}$)$_2$CO]BAr^{F}_{4} in C_6D_5Cl at 80 °C. Inset: Zoom-in of hydride resonance.

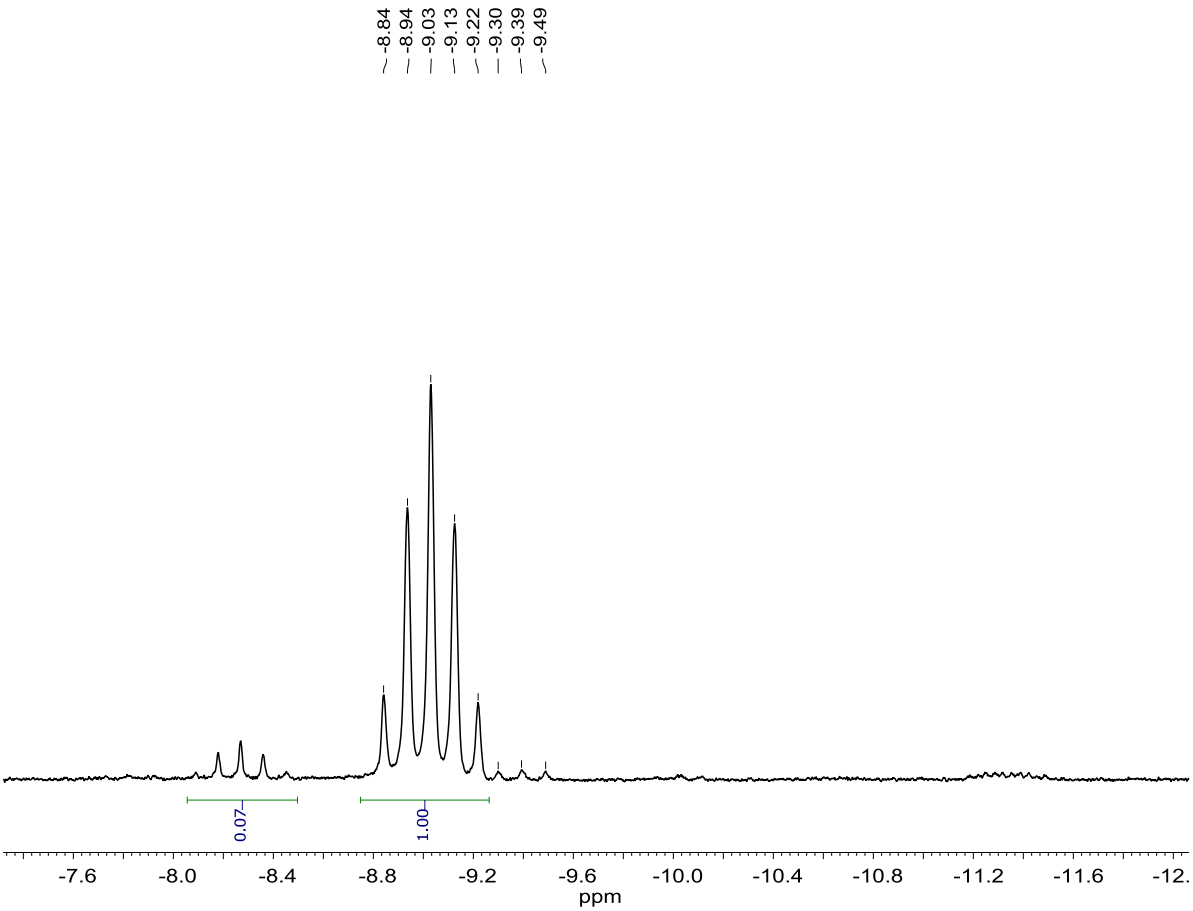

Figure S12. Zoom-in of hydride resonances ^{1}H NMR spectrum of reaction between 2,6-dichloroanilinium BAr^{F}_{4} and *trans*-[HFe($P^{Ph}_{2}N^{Bn}_{2}$)$_2$CO]BAr^{F}_{4} in C_6D_5Cl at 80 °C.

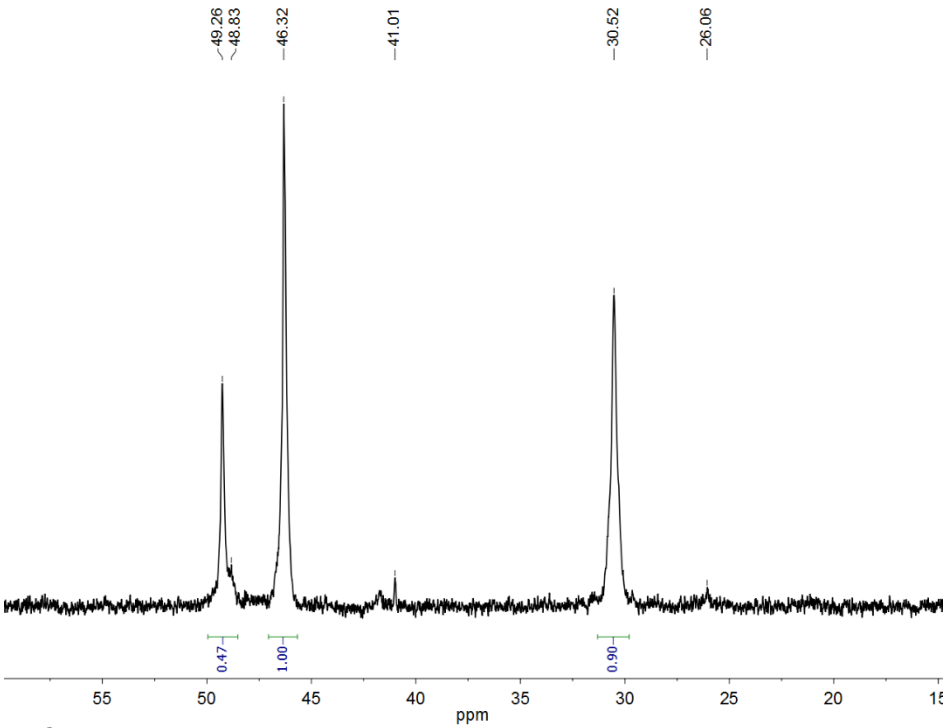

Figure S13. $^{31}P\{^{1}H\}$ NMR spectrum of reaction between 2,6-dichloroanilinium BAr^{F}_{4} and *trans*-$[HFe(P^{Ph}_{2}N^{Bn}_{2})_{2}CO]BAr^{F}_{4}$ in C_6D_5Cl at 80 °C.

.

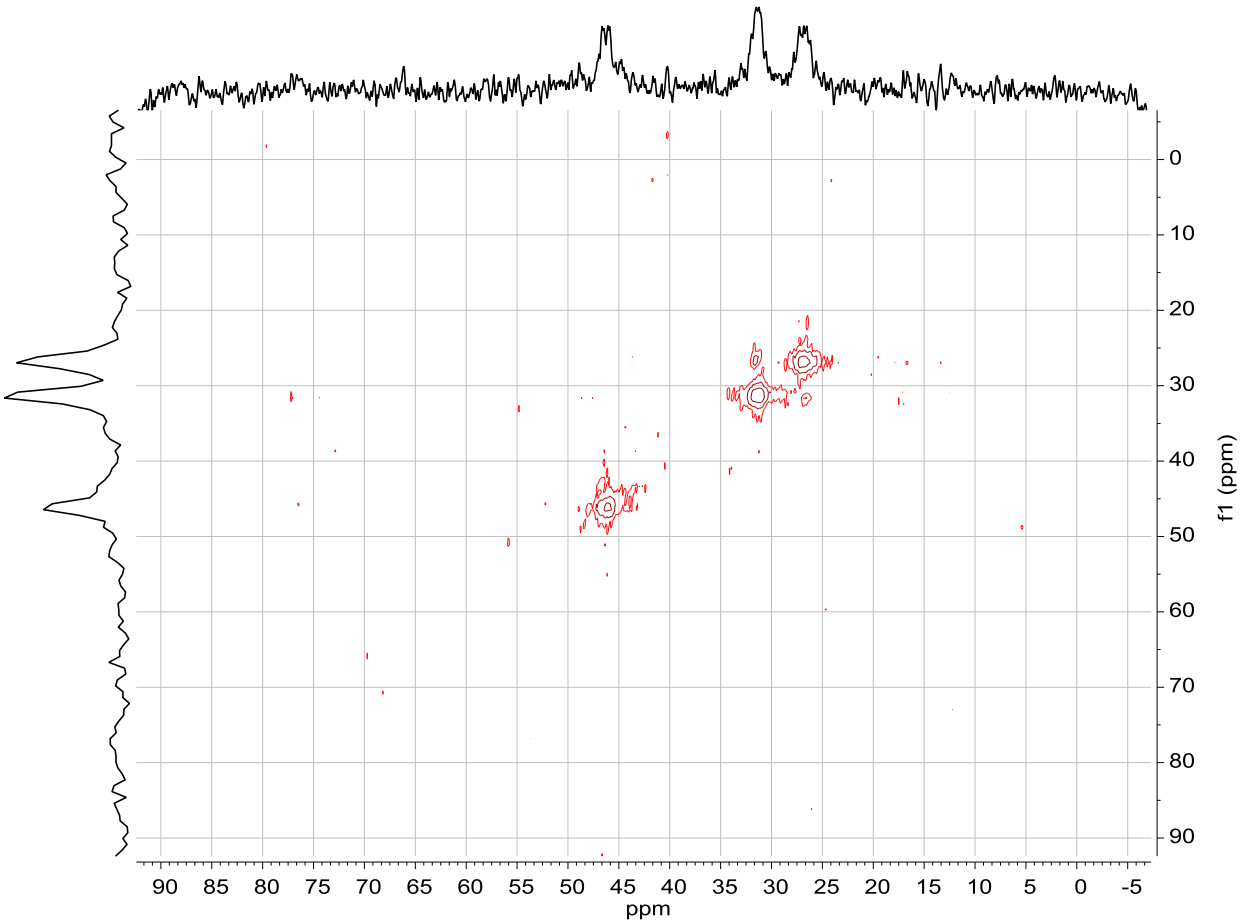

Figure S14. ^{31}P-^{31}P COSY NMR spectrum of reaction between 2,6-dichloroanilinium BAr^{F}_{4} and *trans*-$[HFe(P^{Ph}_{2}N^{Bn}_{2})_{2}CO]BAr^{F}_{4}$ in C_6D_5Cl at -27 °C.

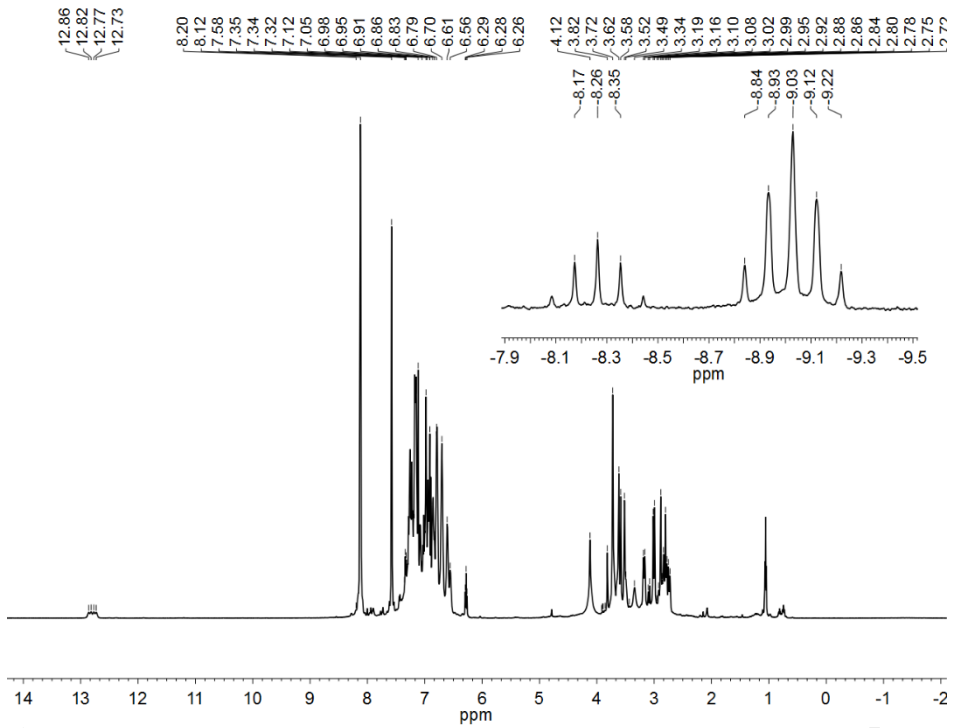

Figure S15. ^{1}H NMR spectrum of reaction between 2,6-dichloroanilinium BAr^{F}_{4} and ^{15}N-labeled *trans*-[HFe($P^{Ph}_{2}N^{Bn}_{2}$)$_2$CO]BAr^{F}_{4} in C_6D_5Cl at 80 °C. Inset: Zoom-in of hydride resonances.

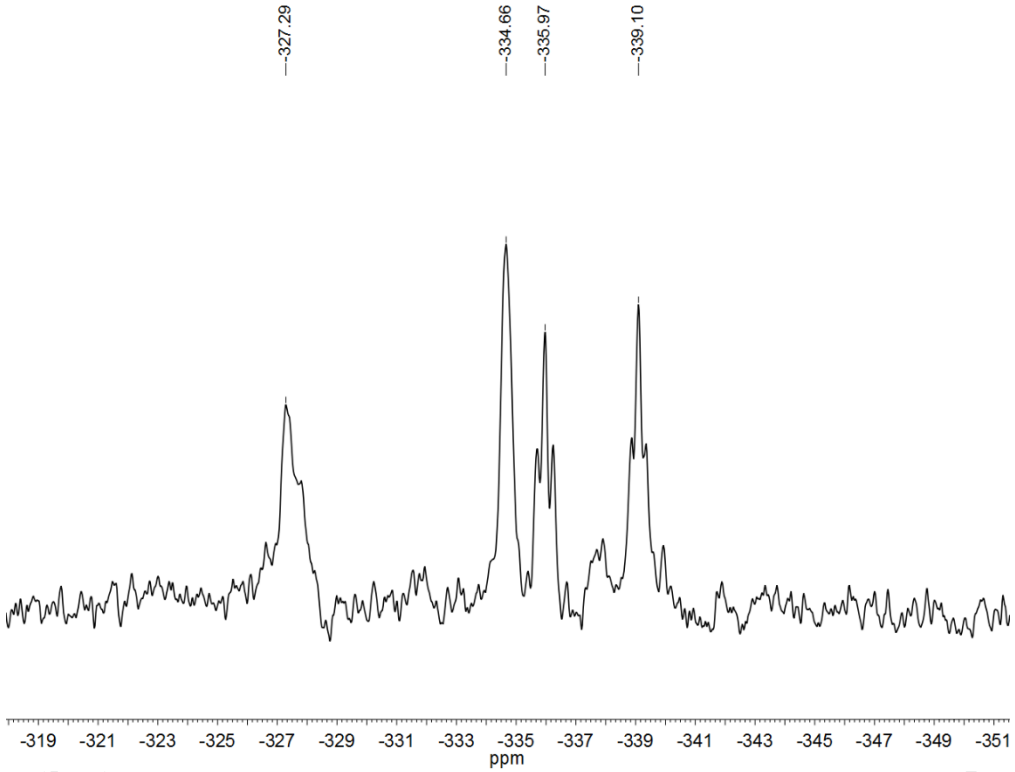

Figure S16. ^{15}N{^{1}H} NMR spectrum of reaction between 2,6-dichloroanilinium BAr^{F}_{4} and *trans*-[HFe($P^{Ph}_{2}N^{Bn}_{2}$)$_2$CO]BAr^{F}_{4} in C_6D_5Cl at 80 °C.

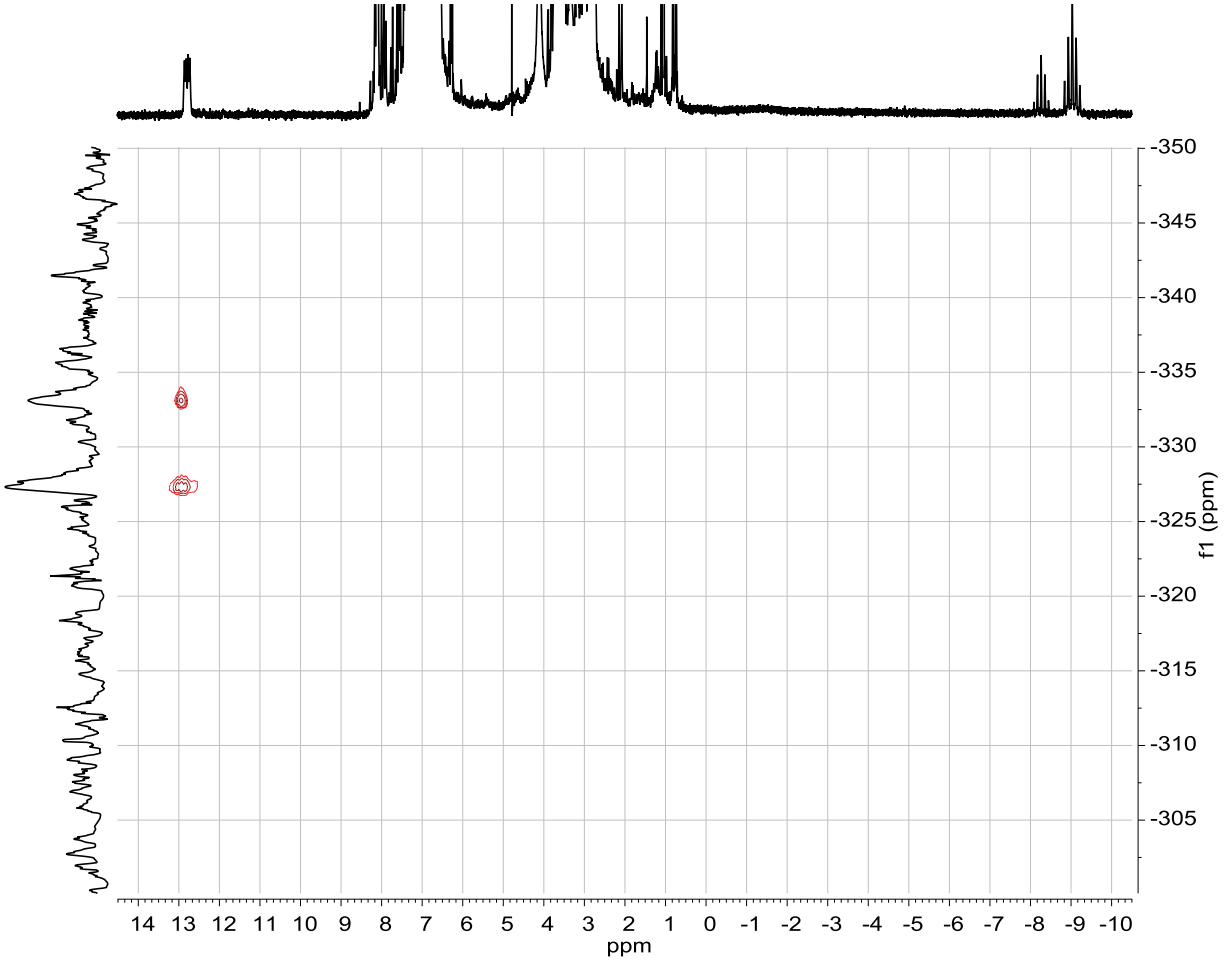

Figure S17. ^{15}N-^{1}H HSQC NMR spectrum of reaction between 2,6-dichloroanilinium BAr^{F}_{4} and *trans*-$[HFe(P^{Ph}_{2}N^{Bn}_{2})_{2}CO]BAr^{F}_{4}$ in C_6D_5Cl at 80 °C.

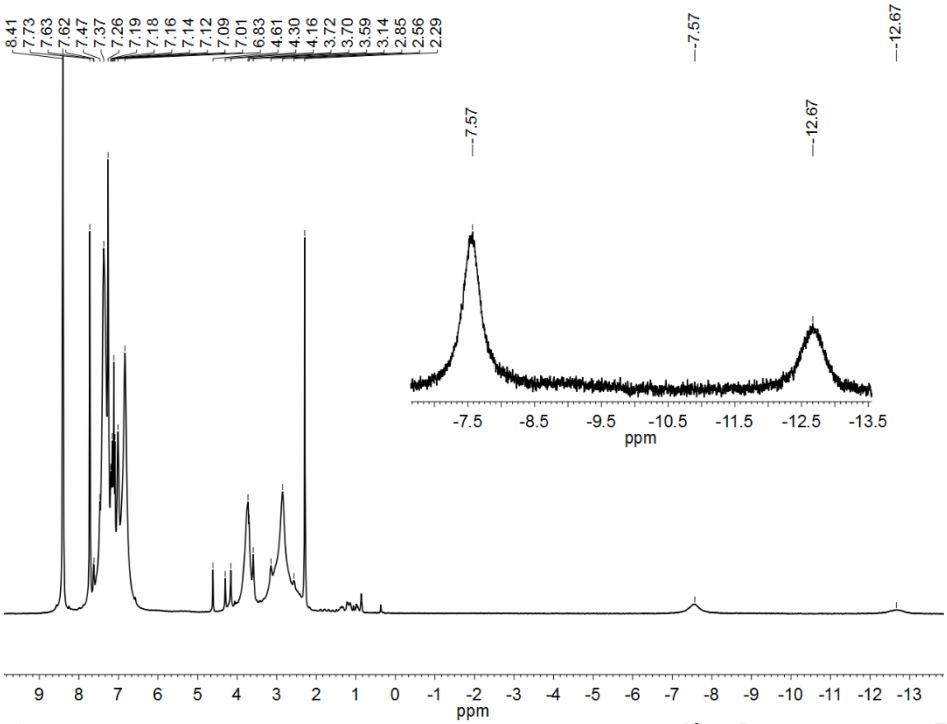

Figure S18. ^{1}H NMR spectrum of reaction between *trans*-HFe($P^{Ph}_2N^{Bn}_2$)$_2$Cl, NaBAr$^{F}_4$, and H_2 in C_6D_5Cl at 20 °C. Inset: Zoom-in of coordinated dihydrogen and hydride resonance.

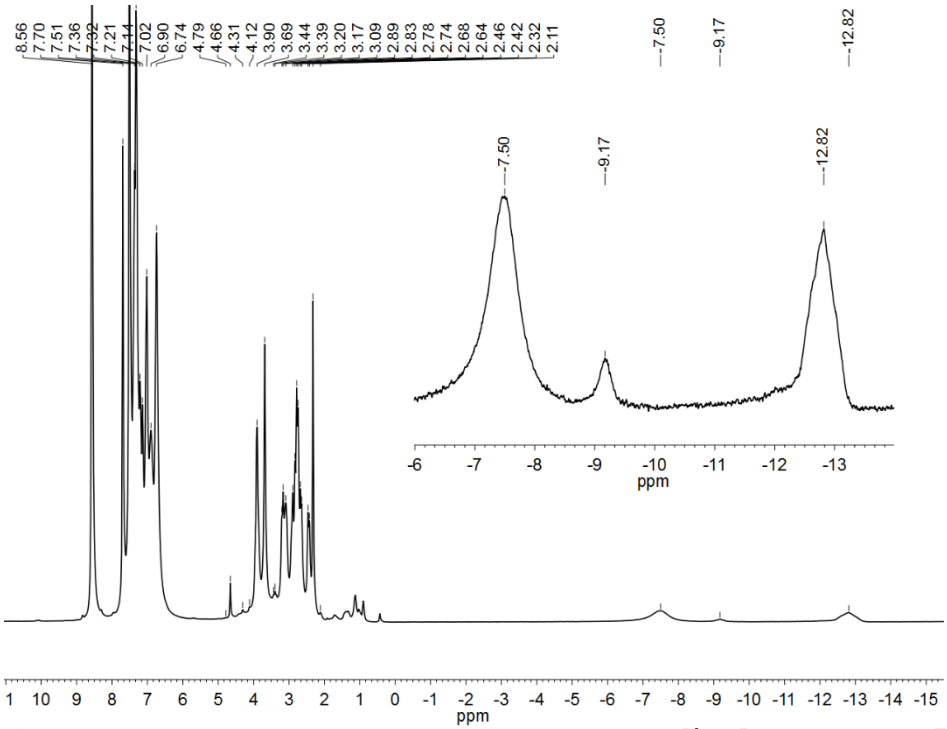

Figure S19. ^{1}H NMR spectrum of reaction between *trans*-HFe($P^{Ph}_2N^{Bn}_2$)$_2$Cl, NaBAr$^{F}_4$, and H_2 in C_6D_5Cl at –30 °C. Inset: Zoom-in of coordinated dihydrogen and hydride resonance.

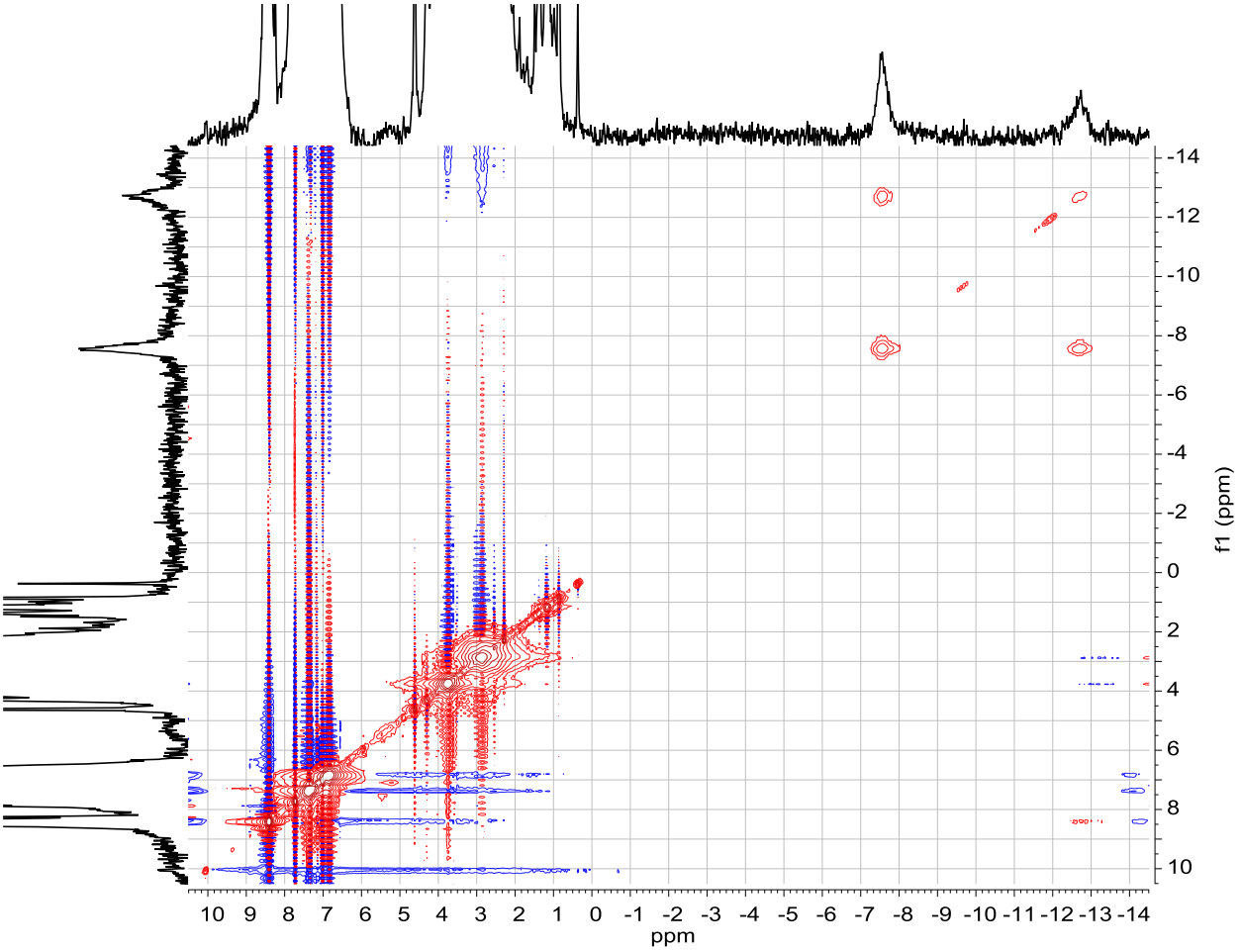

Figure S20. ^{1}H-^{1}H NOESY NMR spectrum with a 25 ms mixing time of the reaction between *trans*-HFe($P^{Ph}_2N^{Bn}_2$)$_2$Cl, NaBAr$^{F}_4$, and H_2 in C_6D_5Cl.

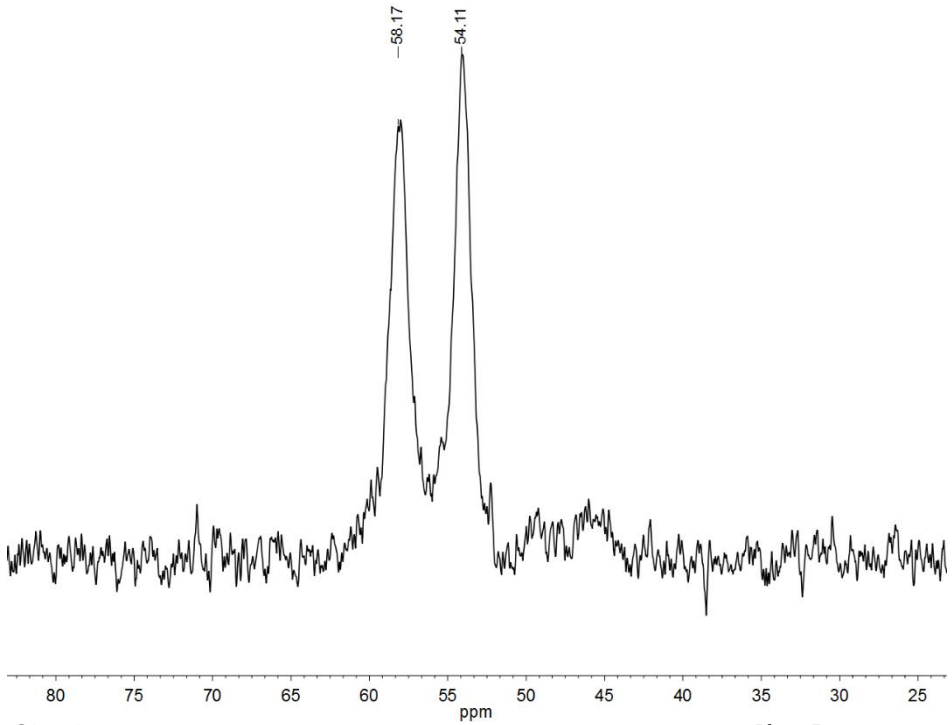

Figure S21. $^{31}P\{^{1}H\}$ NMR spectrum of reaction between *trans*-$HFe(P^{Ph}_2N^{Bn}_2)_2Cl$, $NaBAr^F_4$, and H_2 in C_6D_5Cl at 20 °C.

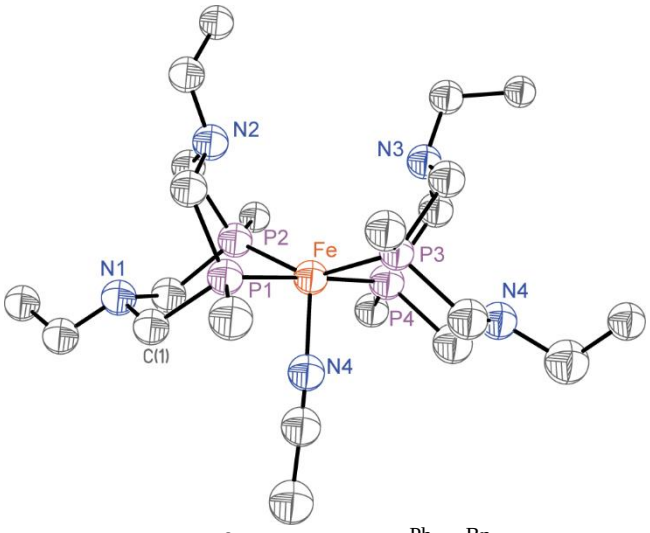

Figure S22. X-ray structural depiction of *trans*-$[HFe(P^{Ph}_2N^{Bn}_2)_2(CH_3CN)]BAr^F_4$. For clarity, the hydrogen atoms are omitted and only the ipso carbon of the phenyl rings are shown. All atoms were refined isotropically and are only to indicate connectivity.

Table S1. Bond distances (Å) and angles (deg) for *cis*-Fe($P^{Ph}_2N^{Bn}_2$)$_2$Cl$_2$

Bond Distances			
Fe(1)-P(1)	2.2126(7)	Fe(1)-Cl(2)	2.3761(7)
Fe(1)-P(2)	2.2660(6)		
Bond Angles			
P(1)-Fe(1)-P(1A)	100.52(4)	P(2)-Fe(1)-P(2A)	169.44(4)
P(1)-Fe(1)-P(2)	93.87(2)	P(2)-Fe(1)-Cl(1)	97.04(2)
P(1)-Fe(1)-P(2A)	79.33(2)	P(2)-Fe(1)-Cl(1A)	90.83(2)
P(1)-Fe(1)-Cl(1)	87.97(2)	Cl(1)-Fe(1)-Cl(1A)	83.74(3)
P(1)-Fe(1)-Cl(1A)	170.92(3)		

Table S2. Selected bond distances (Å) and bond angles (deg) for *trans*-HFe($P^{Ph}_2N^{Bn}_2$)$_2$Cl

Bond Distances			
Fe-P(1)	2.1901(6)	Fe-P(4)	2.1875(6)
Fe-P(2)	2.1513(6)	Fe-Cl	2.4086(5)
Fe-P(3)	2.1697(6)	Fe-H(99)	1.40(3)
Bond Angles			
P(1)-Fe-P(2)	80.25(2)	P(2)-Fe-H(99)	78.3(11)
P(1)-Fe-P(3)	102.09(3)	P(3)-Fe-P(4)	80.55(2)
P(1)-Fe-P(4)	176.02(2)	P(3)-Fe-Cl	100.85(2)
P(1)-Fe-Cl	88.23(2)	P(3)-Fe-H(99)	78.4(11)
P(1)-Fe-H(99)	92.8(11)	P(4)-Fe-Cl	88.34(2)
P(2)-Fe-P(3)	156.60(2)	P(4)-Fe-H(99)	90.6(11)
P(2)-Fe-P(4)	98.55(2)	Cl-Fe-H(99)	178.8(11)
P(2)-Fe-Cl	102.50(2)		

Table S3. Selected bond distances (Å) and bond Angles (deg) for [HFe($P^{Ph}_2N^{Bn}_2$)$_2$CO]BAr$^F_4$

Bond Distances			
Fe(1)-P(1)	2.2110(9)	Fe(1)-P(4)	2.2155(9)
Fe(1)-P(2)	2.1902(8)	Fe(1)-C(61)	1.764(3)
Fe(1)-P(3)	2.1886(8)	Fe(1)-H(99)	1.44(3)
Bond Angles			
P(1)-Fe(1)-P(2)	81.68(3)	P(2)-Fe(1)-H(99)	75.1(1.2)
P(1)-Fe(1)-P(3)	100.25(3)	P(3)-Fe(1)-P(4)	81.29(3)
P(1)-Fe(1)-P(4)	175.84(3)	P(3)-Fe(1)-C(61)	104.7(1)
P(1)-Fe(1)-C(61)	87.9(1)	P(3)-Fe(1)-H(99)	72.6(12)
P(1)-Fe(1)-H(99)	96.2(12)	P(4)-Fe(1)-C(61)	88.5(1)
P(2)-Fe(1)-P(3)	147.64(3)	P(4)-Fe(1)-H(99)	87.9(12)
P(2)-Fe(1)-P(4)	99.11(3)	C(61)-Fe(1)-H(99)	175.8(12)
P(2)-Fe(1)-C(61)	107.7(1)		